Preparation and mechanical properties of composite diamond-like carbon thin films

Q. Wei[a),b),c)]
NSF Center for Advanced Materials and Smart Structures, North Carolina State University, Raleigh, North Carolina 27695, and North Carolina A&T State University, Greensboro, North Carolina 27411

R. J. Narayan
Department of Medicine, Wake Forest University, Winston Salem, North Carolina 27106

A. K. Sharma, J. Sankar,[b)] and J. Narayan[b)]
NSF Center for Advanced Materials and Smart Structures, North Carolina State University, Raleigh, North Carolina 27695, and North Carolina A&T State University, Greensboro, North Carolina 27411

(Received 11 March 1999; accepted 27 August 1999)

We have investigated mechanical properties of diamond-like carbon (DLC) thin films, particularly the internal compressive stress and ways to alleviate it. Foreign atoms such as copper, titanium, and silicon were incorporated into the DLC films during pulsed laser deposition. The chemical composition of the doped films was determined using Rutherford backscattering spectrometry (RBS) and x-ray photoelectron spectroscopy (XPS). Optical microscopy of the doped films showed that DLC films containing Cu exhibit much less particulate density as compared to the films containing Ti and Si. Visible Raman spectroscopy was used to characterize the films. The effect of dopants on the Raman spectrum was analyzed in terms of peak shape and position. Optical microscopy of the pure DLC of a certain thickness showed severe buckling. The mechanisms of adhesion associated with DLC coatings were discussed. Qualitative scratch tests on the specimens showed that pure DLC films have relatively poor adhesion due to a large compressive stress, while the doped DLC films exhibit much improved adhesion. Wear tests show improved wear resistance in the doped DLC coatings. Nanoindentation results suggest that pure DLC has an average hardness above 40 GPa and effective Young's modulus above 200 GPa. The doped DLC films showed slightly decreased hardness and Young's modulus as compared to pure DLC films. These results can be rationalized by analyzing the internal stress reduction as derived from Raman *G*-peak shift to lower wavenumbers. A preliminary interpretation of the stress reduction mechanism is discussed. [S0734-2101(99)05606-7]

I. INTRODUCTION

Carbon manifests itself in several different forms such as diamond, graphite, fullerenes,[1] nanotubes,[2,3] and diamond-like carbon,[4] etc. The various forms of carbon with remarkably diverse properties are a result of its ability to hybridize in several forms such as tetrahedral (sp^3), trigonal (sp^2), and linear coordination (sp^1).[5] The diamond-like carbon (DLC) is an important form of amorphous carbon consisting of a mixture of both sp^3 and sp^2 coordination. It possesses properties close to those of diamond when it consists of a large fraction of sp^3 bonded sites.[6] The attractive properties of this novel structure are high values of hardness, transparency in the infrared range, chemical inertness, and low coefficient of friction and high wear resistance, small electron affinity that leads to field emission effect, etc. Unlike diamond films produced by, for example, hot filament chemical vapor deposition, DLC films are synthesized at much lower temperatures and are usually very smooth. Because of their unique properties, DLC films have found applications as hard protective coatings for magnetic disk drives, as antireflective coatings for IR windows,[7] as field emission source for emitters, and so on.

A number of investigations have corroborated that ultraviolet (UV) pulsed laser ablation of a high purity polycrystalline graphite target is able to produce high quality DLC films with a Tauc gap of ~1.8–2.0 eV and an sp^3/sp^2 ratio of ~80%.[8–10] The interesting aspect of pulsed laser ablation is that it is a nonequilibrium process and the species produced in the laser plasma possess very high kinetic energy. For instance, the kinetic energy of atomic species produced by electron beam evaporation is around ~kT (~0.025 eV at ambient temperature) (k is the Boltzmann constant and T is the absolute temperature) whereas those produced by pulsed laser may be as high as 100–1000 kT (~2.5–25 eV) or even higher.[11] The photon energy might help promote one of the $2s$ electrons to the $2p$ orbital and lead to the formation of sp^3 hybridization that is the precursor of diamondlike carbon constituents. Also, pulsed laser deposition (PLD) can produce hydrogen free DLC films. Upon optimization, PLD produces DLC films superior to filtered cathodic vacuum arc (FCVA)[12] deposition and mass selected ion beam (MSIB) deposition.[13]

However, successful preparation and application of DLC films have long suffered by a large internal compressive

a)Electronic mail: qwei@eos.ncsu.edu
b)Also at Department of Materials Science and Engineering, North Carolina State University, Raleigh, NC 27695-7916.
c)Also at Department of Mechanical Engineering, North Carolina A&T State University, Greensboro, NC 27411.

stress as high as 10 GPa (Ref. 12) in the films regardless of the film growth techniques employed.[14–16] Explanation for the presence of this stress is based upon the subimplantation mechanism of DLC deposition. In this mechanism, incident energetic carbon species bombard the existing DLC film and since usually it takes place at room temperature where mobility of atoms is quite limited, it will give rise to a large compressive stress.[14,17] McKenzie *et al.*[18] even argued that large compressive stress is a prerequisite for the formation of high quality DLC films. Adhesive failure of thin films occurs when the internal stress σ exceeds a critical value. A film of thickness h delaminates when the mechanical energy density exceeds the energy needed to create two new surfaces, such as

$$2G_1\left(\frac{1+\nu}{1-\nu}\right)hf^2<2\gamma, \tag{1}$$

where γ is the surface/interfacial energy, ν the Poisson's ratio, G_1 the shear modulus of the film, and f the strain in the film. If we write the equation in terms of strain, we can have

$$h<\frac{\gamma}{G_1 f^2}\left(\frac{1-\nu}{1+\nu}\right). \tag{2}$$

This equation sets the upper limit on film thickness.

Traditional approaches to obtain DLC films with low internal stress levels involve increasing deposition temperatures or decreasing the energies of carbon species arriving at the substrate surface, etc. Unfortunately, all these are achieved at the expense of reducing sp^3/sp^2 ratio. Anttila *et al.*[19] achieved considerably high adhesion of DLC on silicon by pretreating the silicon surface with ''high energy'' (140 eV) carbon plasma ions. However, the compressive stress of the films introduced during the preparation caused the silicon surface layer to peel off including up to 25 μm thick silicon substrate. Therefore, elimination or minimization of compressive stresses in DLC films offers a major challenge for technological applications of DLC coatings. Some efforts have also been directed toward improving the adhesion of DLC films by depositing an interlayer or several interlayers between the DLC film and the substrate.[20–22].

In this article, we present results on the mechanical properties of pure DLC and DLC films containing various types of dopants prepared by PLD. An ingenious target configuration is used so as to *in situ* incorporate foreign atoms into the DLC films during PLD. The DLC coatings are characterized by RBS, XPS, visible and ultraviolet Raman spectroscopy, optical microscopy, and scratch test for adhesion assessment and wear test for comparison of tribological properties among the specimens. The internal stress reduction is analyzed by observing the Raman peak shift. Nanoindentation measurements are carried out to obtain the Young's modulus and the nanohardness of the DLC films. A preliminary model will be proposed to explain the experimental observations.

II. EXPERIMENTAL PROCEDURE

A. Materials and pulsed laser deposition

The novel target configuration described elsewhere[23] was adopted to incorporate various dopants into DLC films during PLD process. During pulsed laser deposition, the target was spinning and the focused laser beam impinges sequentially on graphite and dopant portions to ablate the target materials to form a composite film. The *p*-type silicon (100) wafers were used as substrates. Copper, titanium, and silicon were chosen as dopants, because a copper interlayer between the substrate and DLC film has been considered to improve the adhesion of the film[21] though Cu is not a carbide former. Ti is a strong carbide former with metallic bonding, and Si is a carbide former with covalent (sp^3) bonding similar to diamond. The Si wafers were cleaned in acetone and methanol ultrasonic baths followed by HF dip to remove the native oxide layer before loading into the laser deposition chamber. The laser beam source used was pulsed excimer laser ($\lambda = 248$ nm, $t_s = 25$ ns) at a repetition rate of 10 Hz, with an energy density close to 3.0 J/cm^2. All the depositions were conducted for 40 min at room temperature in a high vacuum exceeding 10^{-7} Torr.

B. Thin film characterization

Film thickness was measured by a profilometer. The surface morphology of the films was investigated using optical microscopy. Visible Raman spectra were collected using 514 nm coherent photon (laser) beam and were decomposed into two Gaussians to study the peak shift so as to get information on the bonding characteristics and the internal stress reduction. Both RBS and XPS were used for chemical composition determination. Qualitative scratch tests were performed on the specimens to study the adhesion of DLC films on the substrate. The scratches were observed and compared via optical microscopy. A ''crater grinding method'' based upon microabrasion was used to measure the wear resistance of the samples. Nanoindentation measurements were conducted for the Young's modulus and nanohardness of the undoped and doped DLC coatings.

III. RESULTS AND DISCUSSION

First, we will give the film thickness, composition of the doped DLC films as obtained by RBS and XPS, followed by the main features of the Raman spectra of the DLC films. Then, we will present the optical observations on the surface morphology of the undoped and doped DLC films, and we will describe qualitative scratch test results and the morphologies of the scratches. A comparative analysis will be given among the specimens containing different types of dopants. This will be followed by wear resistance results on different specimens. Then results will be given on nanoindentation measurements on doped and undoped DLC coatings. Finally, the mechanical characterization results will be discussed in connection with the internal stress reduction as indicated by the *G*-peak shift in the Raman spectrum.

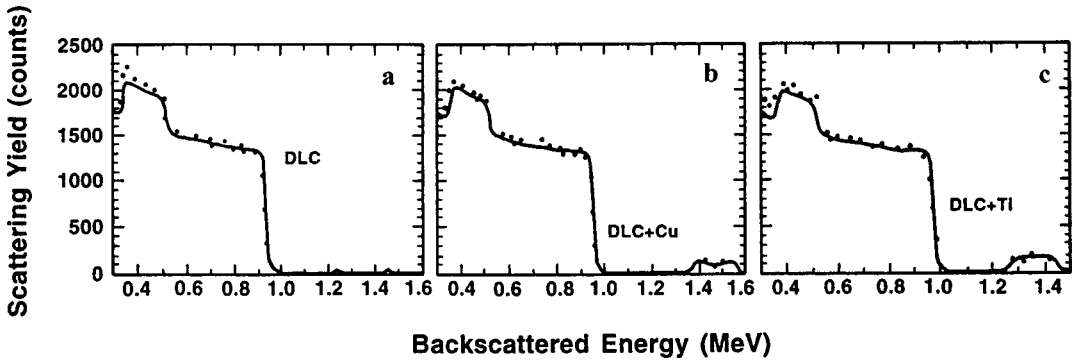

FIG. 1. Rutherford backscattering spectroscopy of pure (a) DLC, (b) DLC+1.2 at. % Cu, and (c) DLC+2.75 at. % Ti.

A. Chemical composition and Raman spectroscopy of composite DLC films

Profilometry on the doped and undoped DLC specimens showed consistently that the film thickness lies in the range of 400–600 nm. Figure 1 shows the RBS results for three samples, i.e., pure DLC, DLC+Cu, and DLC+Ti. Simulations of the RBS results showed that the atomic fraction of Cu in the DLC+Cu film is 1.2% and that of Ti in the DLC+Ti film is 2.75%. Compositional analysis using XPS for these two samples gives 1.44% Cu and 2.66% Ti, respectively, agreeing well with the RBS results.

Composition of the films can be monitored through changing either the position of the laser beam on the target or the size of the metal piece. This will change the perimeter of the circle made by the laser beam on the target surface and the fraction of ablated metal in the circle is therefore changed. The composition can be calculated by extrapolation from geometric consideration calibrated against the composition obtained by, for instance, RBS. The results are given in Table I.

Figure 2 shows the surface morphology of (a) DLC+Cu, (b) DLC+Ti, and (c) DLC+Si. The particulate density in the Cu-doped DLC film is much less than that in Ti and Si-doped DLC films. The shape of these particulates suggests that they were formed out of condensed liquid droplets. The occurrence of particulates is usually attributed to a ''splashing'' mechanism in PLD.[24] It can occur in most materials through substrate boiling (also called true splashing), expulsion of the liquid layer by the shock wave recoil pressure and exfoliation, etc.

The particulate formation during pulsed laser ablation is related to subsurface superheating during laser-solid interaction. The superheating of subsurface layers is controlled by the energy density, absorption coefficient, and thermophysical properties (thermal conductivity, heat capacity, and latent heat) of the substrate.[24] The superheating has been calculated as a function of laser and materials parameters, and correlated with chunk emission. According to this model chunk emission can be minimized and eliminated by controlling laser parameters (optimize energy density for a given laser wavelength) and materials properties (enhancing thermal conductivity and reducing target porosity). These theoretical predictions are found to be in agreement with experimental observations.[24]

For disordered materials such as amorphous Si and Ge that possess the same short range order as their crystalline counterparts, the Raman spectroscopy may be understood on the basis of the selection rule breakdown concept developed by Shuker and Gammon.[25] In a simple approach, the first-order Raman scattering of the amorphous covalent state corresponds to the broadened vibrational density of states. This simple model has been verified in the case of amorphous semiconductors such as Si and Ge.[26] In addition, a Raman peak shift, which can sometimes be observed, is usually attributed to a change of the force-constant values and the broadening of the lines is caused by the relaxation of the **k** selection rules. Since the wavevector **k** corresponds to the eigenvalues of the translational operator in a crystal lattice, therefore it is a good quantum number only for a perfect crystal lattice. In the mean time, the strict selection rules for electronic transitions set by the translational symmetry of the crystal lattice are relaxed and therefore, more modes could contribute to the Raman scattering and result in a broadened Raman spectrum.

So far, experimental Raman spectroscopy of all the tetrahedrally bonded amorphous semiconductors could be explained on the basis of the Shuker–Gammon model. The only exception is carbon.[27] However, we would rather consider DLC not as an exception to Shuker–Gammon model but as a new system. This is because the chemical bonding and short-range order of DLC is much more complicated than the fully tetrahedrally bonded semiconductors. Figure 3

TABLE I. Concentration of dopants in DLC films.

Dopant	Copper			Titanium			Silicon		
Samples	Cu-1	Cu-2	Cu-3	Ti-1	Ti-2	Ti-3	Si-1	Si-2	Si-3
Dopant content	1.4	1.5	2.5	2.7	4.0	7.7	···	···	···

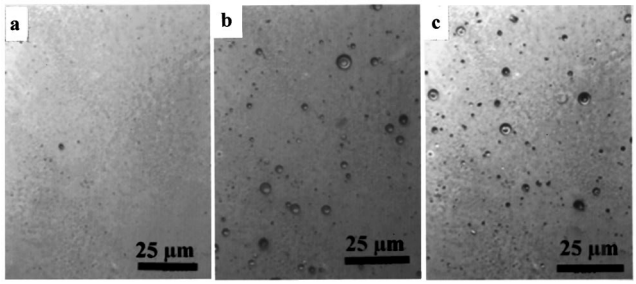

FIG. 2. Optical micrographs of (a) DLC+Cu, (b) DLC+Ti, and (c) DLC+Si. It shows that the particulate density of the Cu-doped DLC is much smaller than those of Ti- and Si-doped DLC.

shows that as is common to all amorphous semiconductors, the distinct sharp peaks are replaced by diffuse, broad peaks due to the relaxation of selection rules for optical transitions. All the spectra show a broad hump centered in the range 1510–1557 cm^{-1}, which is typical of DLC films. This band is associated with optically allowed E_{2g} zone center mode of crystalline graphite (1580 cm^{-1}) and is thus designated as *G* band. There is also a general resemblance between the Raman spectrum of pure DLC, DLC+Cu, and DLC+Si samples. It was argued that a visible Raman spectrum with a relatively symmetrical *G* band corresponds to high sp^3/sp^2 ratio.[28] Apart from the *G* band, the spectra also exhibit a small shoulder at around 1350 cm^{-2} associated with disorder-allowed zone edge mode of graphite and is thus designated as *D* band (A_{1g} mode). It appears that the DLC film doped with Ti shows more asymmetry and an increased *D* band in the Raman spectrum. There is a general tendency in Fig. 3 that all the peak positions of the *G* band of the doped samples have been shifted toward smaller wave number. The shift of Raman peaks will be used to analyze the internal stress reduction in a later section of this article.

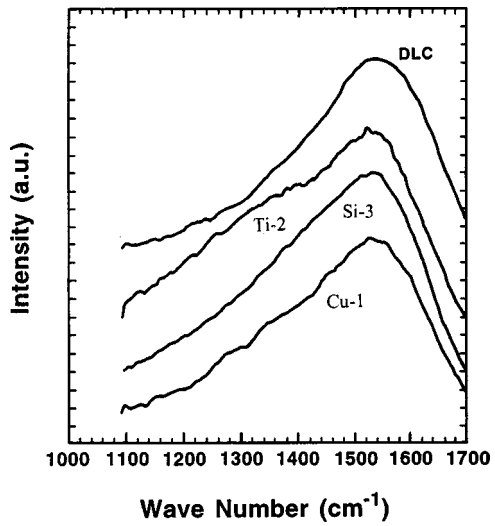

FIG. 3. Visible Raman spectra of pure DLC, DLC doped with Cu, DLC doped with Ti, and DLC doped with Si. The labeling of specimens is referred to Table I.

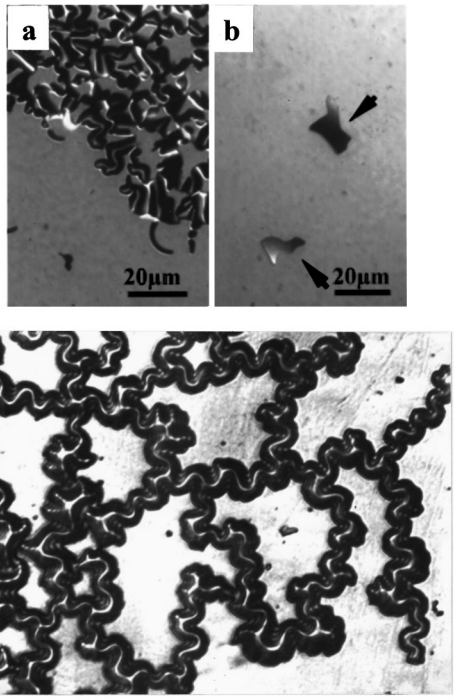

FIG. 4. (a) Peeling off of pure DLC film from the substrate and (b) two flakes of DLC thrown off from the film. (c) Buckling patterns taken from pure DLC film. The buckling exhibits sinusoidal shape. It suggests the poor adhesion of DLC film.

The insignificant effect of Si on the general shape of Raman spectrum could be understood in the light that Si itself is of sp^3 hybridization, being covalently bonded and its presence might not greatly affect the short range environment of DLC structure (bond length and bond angle, for example) that contributes to the Raman spectrum of DLC. In the case of Cu, since its *d* shell is fully occupied and it has been recognized that Cu has little chemical bonding with carbon,[29] it might be expected that Cu would not contribute much to changing the short range environment of DLC either. We have shown[23] in the XPS of Cu in the DLC film that contains Cu two peaks due to Cu $2p_{1/2}$ and Cu $2p_{3/2}$ with binding energies of 952.6 and 933.7 eV, respectively, with no evidence of carbide formation or Cu–C bonding. For XPS of DLC+Ti, however, apart from the peaks corresponding to Ti $2p$ orbital electrons at binding energies of 460 and 454 eV, two shoulders close to them are also observed at 460.9 and 454.7 eV, respectively. These shifts in the binding energies of Ti $2p_{3/2}$(454 eV) and Ti $2p_{1/2}$(460 eV) towards high binding energy side provide evidence of Ti and carbon bonding. The outer shells of a Ti atom is $2d^2 2s^2$, and it might be envisaged that this shell configuration could contribute to the change of short range electronic structure of DLC and thus give rise to the change of Raman spectrum.

B. Adhesion of DLC films

Figure 2 shows the optical micrographs of DLC films containing Cu, Ti, and Si. It is seen that all the doped DLC films stick well to the substrate. No buckling was observed in

these specimens. Figure 4 shows optical micrographs of a pure DLC film with severe buckling [Fig. 4(a)]. Some broken DLC flakes have been thrown off from the surface [Fig. 4(b)]. Usually, buckling would not spread over the whole surface but start from edges of the specimen. At a lower magnification, the sinusoidal shape of the buckling pattern would be more obvious, as shown by Fig. 4(c). The bright contrasts of the sinusoidal wrinkles correspond to the ridges of the buckling. Similar to the observations by Nir,[30] the following behavior of the buckling pattern could be summarized: (a) Stress relief and the buckling process usually begin some time after exposure to air at atmospheric pressure; (b) in most cases, buckling starts at film edges or at defects; (c) the buckling usually develops in a direction perpendicular to film scratches and other defects; (d) the buckling propagates by spreading from a few centers and not by generating new buckling centers; (e) the buckling propagates with a characteristic width; and (f) after propagating a characteristic distance, the buckling undergoes a change in propagation direction or branching.

Theoretically, a thin film heterostructure can be treated as a thin plate attached by adhesive forces to the substrate.[30,31] The appearance of the buckling patterns indicates that DLC films exhibit a very large internal compressive stress. The buckling problem could be treated using the general theory of the buckling of shells and plates that obey Hooke's law. As discussed by Nir,[30] the solution to the buckling equation has a physical meaning as the deflection of the film from the substrate in the normal direction. One type of solution of the buckling equation that is physically meaningful is[31]

$$w = 1 + \cos(kx + qy), \tag{3}$$

where k and q are two constants. This solution implies that the maximum displacement of the ridge formed by the film buckling is along a straight line given by

$$kx + qy = 2n\pi, \quad n = 0, \pm 1, \pm 2, \ldots . \tag{4}$$

The solution consists of two families of parallel ridges crossing each other as described by Eq. (3). Once the buckling process begins, it proceeds in a certain direction. When it reaches a point where two ridges cross each other, it may merge into either of them or branch into both of them.

As pointed out by Iyer *et al.*,[31] for only a small range of internal compressive stresses, the film buckles out with interesting patterns. Smaller stresses could be well accommodated in the film and no relief patterns are observed. For higher stresses, the film cracks or peels off completely. The particular range of stress within which these buckling patterns are observed and their nature depends upon the film-substrate adhesion. Also the buckling is dependent on both the internal compressive stress in the film and the stress at the film-substrate interface. For DLC films, one of the critical variables is the film thickness since the magnitude of the internal compressive stress scales with film thickness. Matsuda *et al.*[32] have studied the dependence of the size of the wrinkles on the film thickness.

It is noted that the buckling phenomenon is absent in all the doped DLC films. It appears that the presence of dopants can reduce the internal compressive stress in DLC films. In order to have a better understanding of how the presence of dopants enhances the adhesion of DLC films, we carried out qualitative scratch tests on pure DLC and some doped DLC films. The term adhesion can mean both the establishment of interfacial bonds and the mechanical load required to break an assembly of heterostructure.[33,34] Because of this, researchers from different fields of study have proposed many theoretical models of adhesion. They include: (1) Mechanical interlocking, (2) electronic theory, (3) theory of boundary layers and interphases, (4) adsorption (thermodynamic) theory, (5) diffusion theory, (6) chemical bonding theory. Among these models, we can usually distinguish between mechanical and specific adhesion, the latter being based on the various types of bonds (electrostatic, secondary, and chemical) that can develop between two solids. In practice, each of these theoretical considerations is valid to some extent, depending upon the nature of the solids in contact and the conditions of formation of the bonded system.

Chemical bonds formed across the coating-substrate interface can greatly participate in the adhesion between two materials. These bonds are generally considered as primary bonds in comparison with physical interactions, such as van der Waals, which are called secondary force interactions. The terms primary and secondary stem from the relative strength or bond energy of each type of interaction. The typical strength of a covalent bond, for example, is on the order of 100–1000 kJ/mol, whereas those of van der Waals interactions and hydrogen bonds do not exceed 50 kJ/mol. It is obvious that the formation and strength of chemical bonds depends upon the reactivity of both coating material and substrate material. In the case of thin film deposition *in vacuo*, one of the key parameters that would considerably affect the chemical bonds between the thin film and the substrate is the surface cleanliness of the substrate prior to deposition and the vacuum condition of the deposition chamber. For instance, if the native oxide of the silicon wafer has not been completely removed prior to the DLC deposition, poor adhesion will usually be observed. On the other hand, fresh Si surface would usually result in good adhesion since Si and C have strong covalent bonding.

A direct measure of adhesion may be obtained by applying a force normal to the interface between the film and substrate.[35] If W is the critical load on the point of radius r, F is the shearing force per unit area due to the deformation of the surface, a is the radius of the circle of contact, and P the indentation hardness of the substrate material, then we can have

$$F = \frac{a \cdot P}{\sqrt{r^2 - a^2}} \quad \text{and} \quad a = \sqrt{\frac{W}{\pi P}}. \tag{5}$$

This shear force is assumed to move an atom of one layer from one equilibrium position to the next and is a direct measure of adhesion. If the distance between the symmetrical equilibrium positions for an atom is x, then $1/2Fx$ would correspond to the height of the potential barrier and therefore the energy of adhesion.

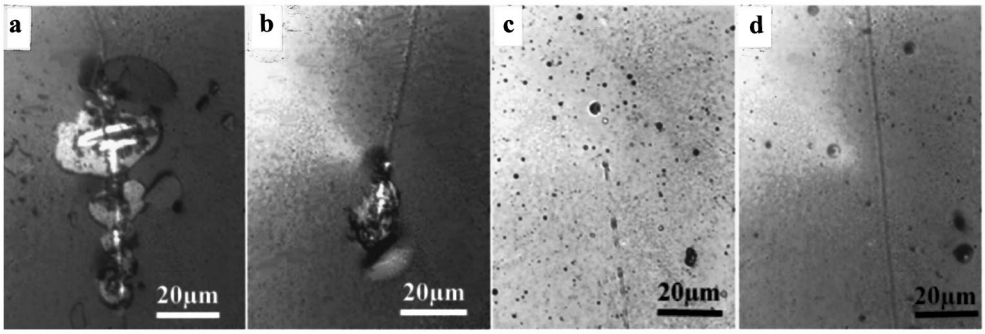

FIG. 5. Optical micrographs of scratches made on pure (a) DLC, (b) DLC+Cu, (c) DLC+Ti, and (d) DLC+Si showing different adhesion properties of these films.

In this study, unlike the purpose of achieving a quantitative critical load, we used a constant normal load of 10 g for all the films and drew the indentor across the film. Qualitative comparison was made between the films by studying the scratch morphology using optical microscopy. Figure 5 shows the scratches made on different diamondlike carbon films. It can be seen that in the case of pure DLC [Fig. 5(a)], the film is easily stripped off from the substrate, indicating poor adhesion. This is consistent with the optical microscopy studies of the buckling patterns of pure DLC film. In all the doped DLC samples, the films adhere well to the substrate [Figs. 5(a)–5(c)], with no buckling patterns. This is particularly true for DLC films containing Ti [Fig. 5(c)] and Si [Fig. 5(d)].

From our results, we conclude that diamond-like carbon films that contain a small content of foreign atoms can have significantly enhanced adhesion. In the pure DLC films, buckling can be frequently observed and the buckling patterns exhibit sinusoidal shape, implying large internal compressive stress in the as deposited film. The geometry and mechanism of the formation of buckling patterns can be described in connection with theories pertaining to the buckling of thin plates or shells. Qualitative scratch tests on the specimens show that DLC films containing foreign atoms exhibit much better adhesion than pure DLC.

C. Wear resistance of DLC coatings

Wear takes place whenever one solid material is slid over the surface of another or is pressed against it. Generally, the tendency of contacting surfaces to adhere arises from the attractive forces that exist between the surface atoms of the two materials. If two surfaces are brought together and then separated, either normally or tangentially, these attractive forces act in such a way as to attempt to pull material from one surface on to the other. The pioneering study on the quantitative aspect of sliding wear by Archard[36] showed that the volume worn away can be written as

$$V = \frac{kLx}{H}, \tag{6}$$

where k is a dimensionless constant dependent on the materials in contact and their exact degree of cleanliness, L is the normal load, x the sliding distance, and H the hardness of the surface being worn away. The constant k is also called wear coefficient analogous to the coefficient of friction. It has been verified that k is always below unity,[37] which suggests that the probability of forming an adhesive wear particle is, in most cases, quite low.

In our study, we use a ''crater grinding method'' based on microabrasion mechanism to acquire the wear resistance of diamondlike carbon coatings. A nominal load of 5 g was applied to create the craters. Figure 6 shows the wear test results for the DLC, DLC+Cu, and DLC+Ti films on silicon. The plots contain the volume worn off (mm^3) as a function of sliding distance (m). Improvement of wear resistance of the DLC films through incorporation of metal is very significant, especially during the initial stages of the wear test. It is also observed that the effect of titanium is stronger than that of copper. One possible reason may be that titanium is a strong carbide former and it produces relatively stronger bonding with carbon in the film, whereas Cu is a very weak carbide former and it is doubtful whether it exists in carbide. This is in accord with our XPS studies as described in Sec. A. What is also apparent from Fig. 6 is that the sliding wear of DLC films follows the Holm–Archard law [Eq. (6)].[36]

The improvement of wear resistance by incorporating foreign atoms into the DLC films is consistent with the enhancement of adhesion of these films by doping. It appears based on our discussions in previous sections that this im-

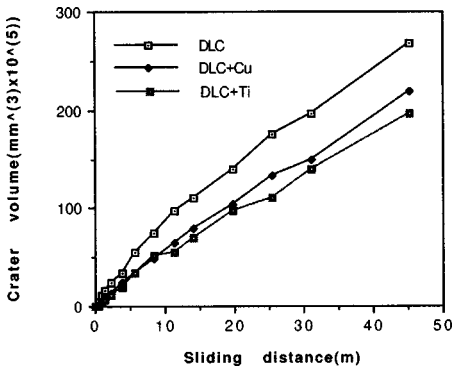

FIG. 6. Wear test results of pure DLC, DLC+Cu, and DLC+Ti.

provement most probably results from reduction in the internal compressive stresses.

D. Nanomechanical characterization of DLC films

Nanoscale mechanical testing of both hydrogen free DLC and hydrogenated DLC has been reported.[38,39] Hoshino *et al.*[39] used ultramicro-indentation method to measure the hardness and Young's modulus of DLC films. The documented hardness value of natural diamond falls in the range 80–102 GPa,[40] but these authors reported for *a*-C:H films hardness values of 200–500 GPa. In their studies of structure and properties of DLC produced by PLD, Voevodin *et al.*[41] showed that the presence of hydrogen reduced film hardness from 60 GPa for *a*-C films to 14 GPa for *a*-C:H films. Savvides and Bell reported a somewhat detailed investigation on the hardness and Young's modulus of diamond and DLC films[38] by nanoindentation. In their experiments, the DLC films were prepared by low energy ion-assisted unbalanced magnetron sputtering. By varying the bombarding ion energy, films were prepared with different sp^3/sp^2 bonding ratio (3–6), optical gaps (1.2–1.6 eV), and hydrogen concentrations (4–20 at. %). The measurements are characterized by substantial elastic recovery, and individual films show a very narrow range of hardness and modulus values. Individual films have mean values of hardness and elastic modulus in the range of 12–30 and 62–213 GPa, respectively.

We have measured the nanohardness and Young's modulus as a function of indentation depth. Figure 7(a) shows the Young's modulus and hardness for undoped pure DLC. It shows Young's modulus above 200 GPa and hardness around 40 GPa. The values of nanoscale mechanical properties represented by Fig. 7(a) imply good film qualities of DLC. It is worth noting that diamond has a Young's modulus of around 1000 GPa and hardness 80–100 GPa, and most of the hard ceramic materials have hardness around or below 20 GPa. It is then clear that our DLC films consist of high percentage of sp^3 bonded carbon. Figure 7(b) gives the nanohardness and Young's modulus of a Cu-doped diamondlike carbon film as a function of indentation depth. It can be seen that, in comparison to undoped DLC, both the Young's modulus and the hardness of the Cu-doped DLC film are slightly reduced.

Figure 7(c) is the nanohardness and Young's modulus of diamondlike carbon film that contains 2.7 at. % Ti. The Young's modulus shows insignificant change as compared to the Cu-doped specimen. However, the nanohardness exhibits slight reduction, with the average value of 25 GPa. It is interesting to recall the scratch test shown in Fig. 5. There it shows that pure DLC exhibits very poor adhesion, indicative of very large internal compressive stress in the film. Figure 5 also shows that the adhesion of DLC containing Cu is not as good as DLC containing Ti and Si. It is envisaged that Cu is not as effective in reducing internal stress as Ti and Si. On the other hand, the Ti-and Si-doped DLC films have substantially reduced internal compressive stresses. However, quantitative information about the internal stress reduction would necessitate further consideration.

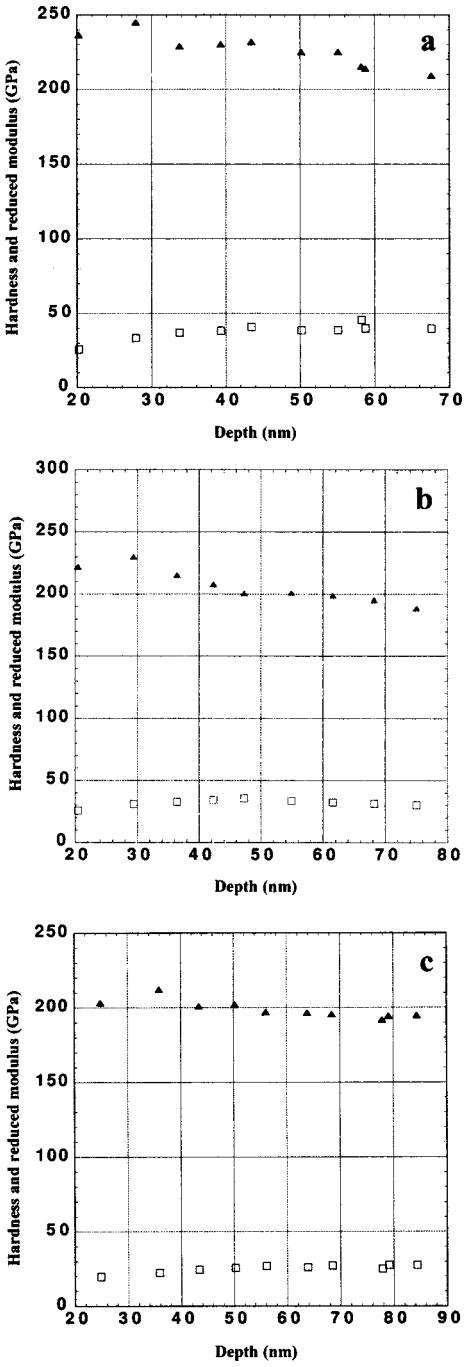

FIG. 7. Nanohardness (squares) and Young's modulus (pyramids) (a) of undoped diamond-like carbon films, (b) of diamond-like carbon film containing 1.4 at. % Cu, (c) and of diamond-like carbon film containing 2.7 at. % Ti as a function of indentation depth.

E. Analysis of internal stress reduction of diamond-like carbon based on Raman spectroscopy

Raman spectroscopy has been used to probe the stress/strain conditions of materials with quite consistent results.[42,43] This is because the stress/strain dependent property is the frequency of the atomic vibrations in a material that can be characterized with the laser Raman spectroscopic technique. The principle by which this technique works is that when a material is stressed, the equilibrium separation

TABLE II. *G*-peak position (cm^{-1}) and internal compressive stress reduction (GPa) as obtained from Raman shift analysis (the *G* peak of pure DLC = 1556.83 cm^{-1}).

Dopant	Copper			Titanium			Silicon		
Samples	Cu-1	Cu-2	Cu-3	Ti-1	Ti-2	Ti-3	Si-1	Si-2	Si-3
$\Delta\sigma$ (GPa)	0.77	1.80	2.31	1.64	4.11	7.2	1.54	1.64	1.67
$(\omega_G - 1500)$ (cm^{-1})	52.03	45.64	42.44	46.60	31.23	11.99	47.24	46.60	46.44

between its constituent atoms is altered in a reversible manner. As a result, the interatomic force constants that determine the atomic vibrational frequencies also change. In general, as the bond lengths increase with tensile load, the force constants and, hence, the vibrational frequencies decrease, while the reverse effect is present when the material is subjected to hydrostatic or mechanical compression. This effect has universal applicability in materials as diverse as commercial polymers, amorphous phases, or inorganics such as silicon.[44–46] The magnitude of the Raman shift can be related to the residual stress, σ, by the following equation:

$$\sigma = 2G \cdot \frac{1+\nu}{1-\nu} \cdot \frac{\Delta\omega}{\omega_0}, \tag{7}$$

where $\Delta\omega$, ω_0, G and ν are the shift in the Raman wave number, the wave number of a reference state, the shear modulus of the material, and the Poisson's ratio of the material, respectively.

In Sec. A, we have presented Raman spectra of some DLC films that are either dopant free or contain some foreign atoms such as Cu, Ti, and Si. In the case of UV Raman spectra, it is observed that the *G*-peak positions located by decomposition of the Raman spectra by multiple Gaussian fitting are 1568.3 cm^{-1} for pure DLC, 1563.6 cm^{-1} for Cu-1, 1560 cm^{-1} for Ti-1, and 1551 cm^{-1} for Si-1 (the labeling of specimen is shown by Table I). The trend is clear that the presence of dopant leads to shift of the *G* peak to smaller wave numbers, indicating that the internal compressive stress of the films is decreased. More detailed analysis is done on the visible Raman data since the Raman spectra can generally be resolved into two Gaussians to achieve the best possible fit. We found significant shift of the *G* peak of the doped DLC films towards lower wave number relative to the undoped DLC. If we use pure DLC as the reference, and use the mechanical properties of DLC as measured by nanoindentation given in the last section, the internal stress reduction can be calculated according to Eq. (7). The results are tabulated in Table II.

It appears that Ti has the strongest effect on internal stress reduction. It is probably because the concentration of Ti is generally higher than Cu. Table II also shows that the effect of Si is somehow constant. This could be understood in terms of the fact that the real concentration of Si has not been changed significantly due to the relatively large density of particulates. Another reason might be that Si is tetrahedrally bonded, and might not be able to contribute significantly to the internal stress reduction in the films. Silicon may also help improve the interfacial adhesion.

The general reduction of internal compressive stress through incorporation of dopants might be understood by invoking the atomic structure of DLC. So far, three models for the atomic structures of DLC have been developed, i.e., the strained layer model, the domain model and the continuous rigid random network (CRN) model.[4] CRN model, which is analogous to amorphous silicon, is the most realistic. The reduction of the internal compressive stresses through the *in situ* introduction of dopants can then be understood on the basis of the effect of these dopants on the CRN of DLC. Transition metals like Cu and Ti are usually more compliant as compared to covalently bonded materials like DLC. The substitution of metal dopants for carbon atoms in the CRN may be able to accommodate or take up the strain by distortion of the electron density distribution since the outer shell electrons of transition metals are loosely bound to the atom. The effect of Si can also be interpreted by the same token.

It is now apparent that appropriate dopants can be used to produce DLC films with reduced internal stresses. The film adhesion can be considerably enhanced. Detailed theoretical modeling is needed to elucidate the underlying mechanism that leads to the stress reduction. Also important is the information of how the dopant atoms are distributed in the CRN of DLC.

IV. SUMMARY AND CONCLUDING REMARKS

Attempts are made to reduce the large internal compressive stresses in the DLC films by *in situ* doping the films with various types of foreign atoms. The mechanical properties of DLC thin films thus made are studied. A novel target design has been adopted to incorporate copper, titanium and silicon into the DLC films during pulsed laser deposition. Optical microscopy of the surface morphology of the doped films showed that DLC films containing Cu exhibit much less particulate density than the films containing Ti and Si. Experimental results of visible Raman spectroscopy are presented and discussed in terms of peak shape and peak position. Optical microscopy of the pure DLC of a certain thickness showed severe buckling of the DLC film. Preliminary scratch tests on the specimens show that pure DLC has quite poor adhesion due to the presence of large compressive stress, while the doped DLC films exhibit much improved adhesion. Wear tests show improved wear resistance in the doped DLC coatings. Nanoindentation results show that pure DLC is of quite good quality, with an average hardness above 40 GPa and Young's modulus above 200 GPa. The

copper-doped DLC films showed slightly decreased hardness and Young's modulus as compared to pure DLC film. Ti and Si can reduce the hardness and Young's modulus more than Cu. All these can be understood by analyzing the internal stress reduction as acquired from Raman *G*-peak shift to lower wave numbers. A preliminary understanding of the stress reduction mechanism is proposed based on outer shell electron distribution distortion as a means of accommodating the internal stress relief.

ACKNOWLEDGMENTS

The authors thank Dr. Ashok for fruitful discussions and help with the nanoindentation measurements. They also thank Dr. Tallant from Sandia National Labs for UV Raman measurements and helpful suggestions. This research is sponsored by the National Science Foundation under Contract CMS No. 9414434.

[1]H. W. Kroto, J. R. Heath, S. C. O'Brien, R. F. Curl, and R. E. Smalley, Nature (London) **318**, 162 (1985).
[2]S. Iijima, Nature (London) **354**, 56 (1991).
[3]*Carbon Nanotubes: Preparation and Properties*, edited by T. W. Ebbesen (CRC Press, Boca Raton, FL, 1997).
[4]J. Robertson, Prog. Solid State Chem. **21**, 199 (1991).
[5]P. W. Atkins, *Physical Chemistry*, 5th ed. (W. H. Freeman and Company, San Francisco, 1994).
[6]W. I. Milne, J. Non-Cryst. Solids **198–200**, 605 (1996).
[7]A. Bozhko, A. Ivanov, M. Berrettoni, S. Chudinov, S. Stizza, V. Dorfman, and B. Pypkin, Diamond Relat. Mater. **4**, 488 (1995).
[8]J. Krishnaswamy, A. Rengan, J. Narayan, K. Vedom, and C. J. McHorgue, Appl. Phys. Lett. **54**, 2455 (1989).
[9]T. Sato, S. Furuno, S. Ifuchi, and M. Hanabusa, Jpn. J. Appl. Phys., Part 1 **26**, 1487 (1987).
[10]D. L. Pappas, K. L. Saenger, J. Bruley, W. Krakow, and J. J. Cuomo, J. Appl. Phys. **71**, 5672 (1992).
[11]E. A. Rohlfing, J. Chem. Phys. **89**, 6103 (1988).
[12]M. Chhowalla, Y. Yin, G. A. J. Amaratunga, D. R. McKenzie, and Th. Frauenheim, Diamond Relat. Mater. **6**, 207 (1997).
[13]J. Kulik, Y. Lifshitz, G. D. Lempert, J. W. Rabalais, and D. Marton, J. Appl. Phys. **76**, 5063 (1994).
[14]D. Nir, Thin Solid Films **146**, 27 (1987).
[15]M. Weiler, S. Sattel, T. Giessen, and K. Ehrhardt, Phys. Rev. B **53**, 1594 (1996).
[16]J. P. Sullivan, T. A. Friedmann, and A. G. Baca, J. Electron. Mater. **26**, 102 (1997).
[17]P. Koidl, C. Wild, B. Dischler, J. Wagner, and M. Ramsteiner, Mater. Sci. Forum **52–53**, 41 (1989).
[18]D. R. McKenzie, D. Muller, and B. A. Pailthorpe, Phys. Rev. Lett. **67**, 773 (1991).
[19]A. Anttila, J. Salo, and R. Lappalainen, Mater. Lett. **24**, 153 (1995).
[20]M. Crischke, K. Bewilogua, K. Trojan, and H. Dimigen, Surf. Coat. Technol. **74–75**, 739 (1995).
[21]M. D. Bentzon, K. Mogensen, J. B. Hansen, C. Barholm-Hansen, C. Taholt, P. Holiday, and S. S. Eskildsen, Surf. Coat. Technol. **68–69**, 651 (1994).
[22]J. Narayan, R. D. Vispute, and K. Jagannadham, J. Adhes. Sci. Technol. **9**, 753 (1995).
[23]Q. Wei, R. J. Narayan, J. Narayan, J. Sankar, and A. K. Sharma, Mater. Sci. Eng., B **53**, 262 (1998).
[24]R. K. Singh, D. Bhattacharya, and J. Narayan, Appl. Phys. Lett. **57**, 2022 (1990).
[25]R. Shuker and R. W. Gammon, Phys. Rev. Lett. **25**, 222 (1970).
[26]R. A. Street, *Hydrogenated Amorphous Silicon* (Cambridge University Press, Cambridge, 1991).
[27]V. Paillard, P. Melinon, V. Dupuis, A. Perez, J. P. Perez, G. Guiraud, J. Fornazero, and G. Panczer, Phys. Rev. B **49**, 11433 (1994).
[28]D. R. Tallant, T. A. Friedmann, N. A. Missert, M. P. Siegal, and J. P. Sullivan, Mater. Res. Soc. Symp. Proc. **498**, 37 (1998).
[29]P. M. Hansen, *Constitution of Binary Alloys* (Wiley, New York, 1958).
[30]D. Nir, Thin Solid Films **112**, 41 (1984).
[31]S. B. Iyer, K. S. Harshavardhan, and V. Kumar, Thin Solid Films **256**, 94 (1995).
[32]N. Matsuda, S. Baba, and A. Kinbara, Thin Solid Films **81**, 301 (1981).
[33]J. Schultz and M. Nardin, in *Handbook of Adhesion Science and Technology*, edited by D. E. Packhaw (Wiley, New York 1992), pp. 19–33.
[34]K. W. Allen, 10th Annual Meeting of The Adhesion Soc., Inc., Williamsburg, Virginia, 22–27 February, 1987.
[35]C. Weaver, *Proceedings of the 1st International Conference on Vacuum Technology* (Pergamon, New York, 1958).
[36]J. F. Archard, J. Appl. Phys. **24**, 981 (1953).
[37]E. Rabinowicz, *Friction and Wear of Materials*, 2nd ed. (Wiley, New York, 1995).
[38]N. Savvides and T. Bell, J. Appl. Phys. **72**, 2791 (1992).
[39]S. Hoshino, K. Fujii, N. Shohata, H. Yamaguchi, Y. Tsukamoto, and M. Yanagisawa, J. Appl. Phys. **65**, 1918 (1989).
[40]C. A. Brooks, in *The Properties of Diamond*, edited by J. E. Field (Academic, New York, 1979), p. 383.
[41]A. A. Voevodin *et al.*, J. Vac. Sci. Technol. A **14**, 1927 (1996).
[42]C. Galiotis, Mat. Tech. **8**, 203 (1993).
[43]L. S. Schadler and C. Galiotis, Int. Mater. Rev. **40**, 116 (1995).
[44]I. M. Robinson, M. Zakikhani, R. J. Day, R. J. Young, and C. Galiotis, J. Mater. Sci. Lett. **6**, 1212 (1987).
[45]N. Melantitis and C. Galiotis, J. Mater. Sci. **25**, 5081 (1990).
[46]X. Yang and R. J. Young, Composites **25**, 488 (1994).